



Konrad Dadej*, Jarosław Bieniaś, Barbara Surowska

Lublin University of Technology, Faculty of Mechanical Engineering, Department of Materials Engineering, ul. Nadbystrzycka 36, 20-618 Lublin, Poland

*Corresponding author. E-mail: k.dadej@pollub.pl

Received (Otrzymano) 26.08.2017

INTERLAMINAR CRACKING RESISTANCE OF NONHOMOGENEOUS COMPOSITE BEAMS

This article is devoted to interlaminar cracking research on carbon multidirectional fibrous-epoxy composites. Composite beams with $0^\circ/0^\circ$, $0^\circ/45^\circ$ and $0^\circ/90^\circ$ interfaces were subjected to double cantilever beam tests whereby force-crack opening displacement curves were determined. Additionally, crack length observations were conducted in order to determine the crack resistance curves of multidirectional composites. On the basis of the performed tests, it was found that the critical strain energy release rate for crack initiation is size independent of the material configuration. On the other hand, the fiber orientation is crucial to the critical strain energy release rate for crack propagation.

Keywords: interlaminar fracture toughness, asymmetric double cantilever beam, multidirectional laminates, beam theory

ODPORNOŚĆ NA PĘKANIE MIĘDZYWARSTWOWYCH NIEHOMOGENICZNYCH BELEK KOMPOZYTOWYCH

Artykuł dotyczy badań odporności na pękanie wielokierunkowych kompozytów epoksydowo-włóknistych na bazie włókien węglowych. Belki kompozytowe z interfejsami $0^\circ/0^\circ$, $0^\circ/45^\circ$ oraz $0^\circ/90^\circ$ zostały zbadane za pomocą metody Double Cantilever Beam, w których wyznaczono charakterystyki siła - wielkość rozwarcia szczeliny. Dodatkowo prowadzono obserwacje długości pęknięcia w celu wyznaczenia krzywych odporności na pękanie kompozytów wielokierunkowych. Na podstawie przeprowadzonych badań stwierdzono, że wartość krytycznego współczynnika uwalniania energii dla inicjacji pęknięcia jest wielkością niezależną od ukierunkowania włókien. Natomiast ułożenie włókien jest kluczowe w przypadku krytycznego współczynnika uwalniania energii dla propagacji pęknięcia.

Słowa kluczowe: międzywarstwowa odporność na pękanie, teoria belek, asymetryczne podwójne wsparcie belek, laminaty wielokierunkowe

INTRODUCTION

The damage mechanisms of fiber reinforced polymers (FRP) are characterized by failure forms which do not occur in classical monolithic materials. The following forms of failure are distinguished in laminates: longitudinal tensile and compression failure of the matrix and fibers [1, 2], transverse matrix cracks in the composite ply without fiber failure - intralaminar fracture [3]; delaminations between differently oriented plies - interlaminar fracture [4-6]. Material resistance for delamination initiation and growth between laminate plies is usually investigated in interlaminar fracture toughness (IFT) tests. The characteristic feature of this kind of tests is beam-shaped specimens which are especially loaded to obtain one of the three fracture modes - mode I (opening), mode II (shearing) or mode III (anti-plane shearing). In IFT tests critical strain energy release rates (SERR), are determined - the critical amount of energy which can be accumulated in loaded material. Crack propagation occurs after the

internal energy reaches its critical value. The energy is dissipated during development of the new surface area caused by crack growth. IFT tests are commonly performed on classical unidirectional fibrous composites by the double cantilever beam (DCB) method for mode I [7, 8]. Determining SERR in pure mode II is generally conducted by means of the end notched flexure test (ENF) [5, 8-10]. On the other hand, the SERR of composite materials in mode III is rarely studied. Furthermore, IFT tests resulting in mode mixing conditions at the crack tip are increasingly investigated [11]. A summary of IFT research issues for multidirectional composites was presented by Andersons and Konig [11].

Literature analysis indicates that most interlaminar fracture toughness tests performed on multidirectional laminates by means of DCB and ENF methods are considered as pure mode I or mode II. However, some research on the crack propagation phenomena in multidirectional laminates has proved that the above men-

tioned test conditions will always result in mode mixity at the crack tip (when delamination lies on the interface between various oriented layers) [5, 12]. Therefore it is necessary to determine not only the total critical strain energy release rate for considering an angular interface, but also the quantitative contribution of opening/shear mode at the crack tip. In this paper, experimental tests of multidirectional laminates were performed. The experimental observations and results were subjected to further analytical calculations by means of the recent enhanced beam theory [13] to determine the SERR of multidirectional composite material from an asymmetrical beam specimen. The aim of this paper was to determine the influence of the interface fiber orientation on the critical strain energy release rate, taking into account the mode I and mode II contributions at the crack tip.

METHODOLOGY

Material

Experimental asymmetrical DCB tests were performed on multidirectional composite laminates. The scheme and geometrical dimensions of the manufactured test specimens are presented in Figure 1.

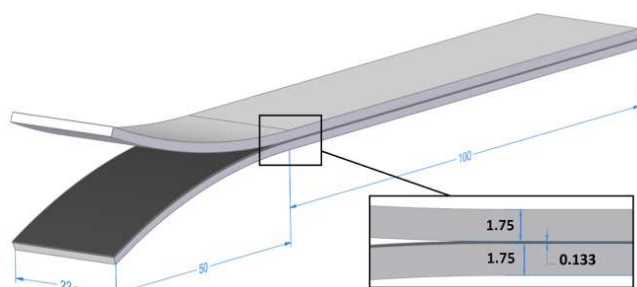


Fig. 1. Specimen geometry of multidirectional $0^\circ/45^\circ$ and $0^\circ/90^\circ$ laminates

Rys. 1. Geometria próbek wielokierunkowych laminatów w układach $0^\circ/45^\circ$ i $0^\circ/90^\circ$

Specimens in symmetrical configuration $0^\circ/0^\circ$ were manufactured from 28 layers of unidirectional prepregs. The total thickness of the specimens was 3.8 mm. In this case, the delamination was located in exactly half the thickness of the beam. On the other hand, the asymmetrical specimens (Fig. 1) were manufactured with 26 layers of unidirectional prepreg in 0° orientation and an additional off-axis layer oriented at 45° and 90° according to the specimen longitudinal axis. Specimens were manufactured in such a way as to obtain a similar thickness of reinforcing layers oriented at 0° (Fig.1) as well as to obtain similar extensional and bending stiffnesses of the sublaminates separated by the delamination. For that reason, the delamination was 0.133 mm from the specimen centerline, creating a $0^\circ/\varphi$ interface, as shown in Figure 1.

The nominal fibre content was about 60% of volume. The material was manufactured by the autoclaving method (Machinenbau Scholz, Germany) in the Department of Materials Engineering at Lublin University of Technology. The following autoclave process parameters were applied: curing temperature 135°C , curing time 2 h, heating and cooling gradient $2^\circ\text{C}/\text{min}$, pressure 4.5 bar, underpressure -0.8 bar. The mechanical properties of the carbon fiber reinforced polymer unidirectional material are presented in [5].

Enhanced Beam Theory

Valvo [13] proposed the enhanced beam theory, which is based on the specimen theoretical division. The specimen for IFT tests is virtually divided into three parts, which are characterized by their own stiffness and compliances. Knowing the forces on the specimen crack tip, the total strain energy release rate can be calculated, as well as the mode I and II contributions [13]:

$$G = \frac{1}{2B} \left[\frac{f_{\varphi M} \rho_u^2 - (f_{\varphi N} + f_{uM}) \rho_u \rho_\varphi + f_{uN} \rho_\varphi^2}{f_{uN} f_{\varphi M} - f_{uM} f_{\varphi N}} + \frac{\rho_w^2}{f_{wQ}} \right] \quad (1)$$

$$G = G_I + G_{II} \quad (2)$$

$$G_I = \frac{1}{2B} \left[\frac{1}{f_{uN}} \frac{(f_{uN} \rho_\varphi - f_{\varphi N} \rho_u + f_{\varphi N} \rho_\varphi)^2}{f_{uN} f_{\varphi M} - f_{uM} f_{\varphi N}} + \frac{\rho_w^2}{f_{wQ}} \right] \quad (3)$$

$$G_{II} = \frac{1}{2B} \frac{\rho_u^2}{f_{uN}} \quad (4)$$

where ρ_u is the crack-tip sliding displacement rate, ρ_w is the crack-tip opening displacement rate and ρ_φ is the crack tip relative rotation rate. f_{uN} , f_{uM} , $f_{\varphi N}$, f_{wQ} , $f_{\varphi M}$ are the flexibility coefficients of the sublaminates. The above mentioned parameters are described in detail in Valvo paper [13] and can be calculated in terms of classical laminate theory (CLT) [14].

Knowing the mode I and mode II contributions at the crack tip, the mode mixity ratio can be calculated based on the Hutchinson and Suo method [15]:

$$\psi = \arctan \sqrt{\frac{G_{II}}{G_I}} \quad (5)$$

Classical Laminate Theory

The values of flexibility coefficients f_{uN} , f_{uM} , $f_{\varphi N}$, f_{wQ} , $f_{\varphi M}$ are necessary to determine the strain energy release rates by means of EBT. The above mentioned coefficients are functions of sublaminates compliances [5, 13, 14], which can be calculated as follows:

$$a_\alpha = \frac{D_\alpha}{A_\alpha D_\alpha - B_\alpha^2}; \quad b_\alpha = \frac{B_\alpha}{A_\alpha D_\alpha - B_\alpha^2}; \quad c_\alpha = \frac{1}{C_\alpha}; \quad d_\alpha = \frac{A_\alpha}{A_\alpha D_\alpha - B_\alpha^2} \quad (6)$$

where $A_\alpha, B_\alpha, C_\alpha, D_\alpha$ are respectively the *extensional stiffness, bending-extension coupling stiffness, shear stiffness, and bending stiffness*, per unit width. According to CLT [14], a asymmetrical and nonhomogeneous beam can be treated as homogeneous, when equivalent stiffnesses are known [5, 14]. The sublaminata stiffnesses $A_\alpha, B_\alpha, C_\alpha, D_\alpha$ ($\alpha \in 1,2,3$) can be computed as follows:

$$A_\alpha = \sum_{i=1}^n E_x^{(i)}(z_k - z_{k-1}) \quad (7)$$

$$B_\alpha = \frac{1}{2} \sum_{i=1}^n E_x^{(i)}(z_k^2 - z_{k-1}^2) \quad (8)$$

$$C_\alpha = \frac{5}{6} \sum_{i=1}^n G_{zx}^{(i)}(z_k - z_{k-1}) \quad (9)$$

$$D_\alpha = \frac{1}{3} \sum_{i=1}^n E_x^{(i)}(z_k^3 - z_{k-1}^3) \quad (10)$$

Where z_k are lamina coordinates which indicate the distance between the laminate centerline and a particular lamina interface, as shown in Figure 2 [14].

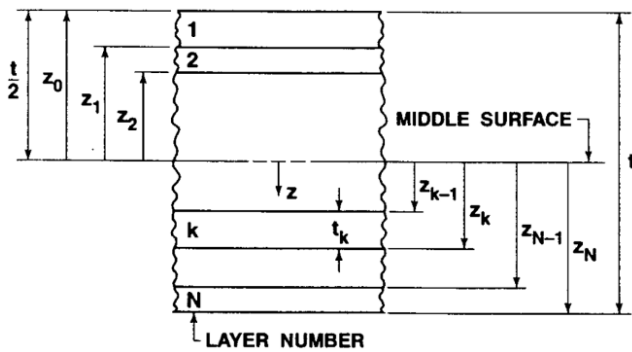


Fig. 2. Theoretical division of N layered composite laminate [14]
 Rys. 2. Teoretyczny podział laminatu składającego się z N warstw [14]

RESULTS AND DISCUSSION

Figure 3 presents representative *force (P) - crack opening displacement (COD)* curves of the tested materials. Firstly, a linear force increase can be observed as a function of COD. The highest specimen stiffness was observed for the $0^\circ/0^\circ$ configuration, while specimens with the $0^\circ/45^\circ$ and $0^\circ/90^\circ$ interface were characterized by a similar slope of the *P-COD* curve. Generally, it can be observed, that the *P-COD* curves are similar for crack growth on interfaces $0^\circ/0^\circ$ and $0^\circ/45^\circ$, while the $0^\circ/90^\circ$ interface is characterized by higher force levels.

According to ASTM Standard 5528 [16], the nonlinearity onset in *P-COD* characteristics is marked by the 'NL point'. That first point of nonlinearity is frequently used to describe crack growth initiation in the IFT test. This NL point indicates crack propagation onset, which has an influence on beam compliance. Delamination growth by value Δa results in higher compliance of a DCB specimen.

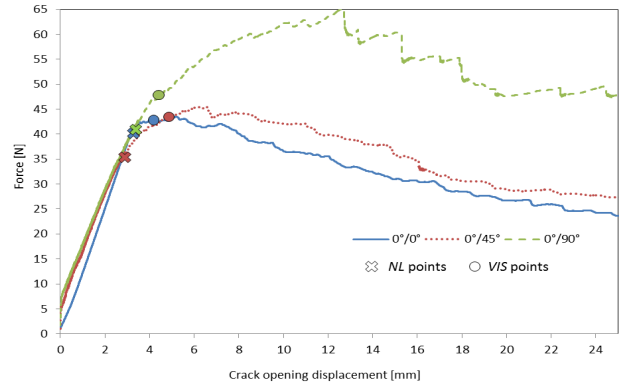


Fig. 3. Force-crack opening displacement curve for multidirectional laminates

Rys. 3. Krzywe siła-wielkość rozwarcia szczeliny dla wielokierunkowych laminatów

A different crack initiation criterion is indicated by the VIS point [16]. This point indicates the force and COD levels when crack growth can be macroscopically observed on the specimen edge. In this article a crack increase of 1 mm was applied to determine the VIS point. To determine the VIS point and then calculate SERR for that criterion, on-line observation of the crack length coupled with the *P-COD* curve is necessary. The calculated SERR value for specified crack length $a_0 + \Delta a$ allows the *R-curve* (Fig. 4) to be determined, which describes the crack resistance characteristics of the composite material as a function of crack length.

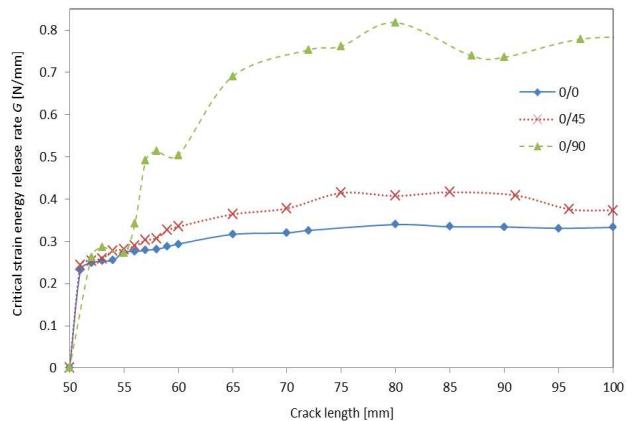


Fig. 4. R-curves for various interfaces of carbon fiber reinforced polymer

Rys. 4. Krzywe oporu pęknięcia dla różnych interfejsów kompozytu epoksydowo-węglowego

The idea of determining the *R-curves* of the material is connected with the bridging effect of fibers - a different energy value is dissipated by the crack onset, and by the crack propagation where the reinforcing fibers couple the two composite surfaces created by the crack increase. The increase in SERR as a function of crack length is associated with incomplete fiber-matrix separation. This effect causes the total energy delivered to the specimen to be partly dissipated by the crack growth and partly consumed by the bending of the two cantile-

ver beams and the stretching and bending of the coupling bridging fibers [17, 18].

In the case of the $0^\circ/0^\circ$ configuration, the *R-curve* after about a 20 mm crack growth, stabilizes at the level about 0.35 N/mm, which indicates that after this specified crack increase, a balance is achieved between the bridging fibers breakage rate and crack growth rate. Generally, configuration $0^\circ/0^\circ$ is characterized by stable crack growth, as well as a straight and smooth propagation path, which is shown in Figure 5A. When analyzing the *R-curve* for interface $0^\circ/45^\circ$, similar stabilization of SERR after about a 20 mm crack growth can be observed, as for $0^\circ/0^\circ$. However, in this case additional fluctuations of the SERR values can be observed between about 25 and 40 mm of crack increase. These fluctuations can be caused by creating a large scale bridging effect, and then by crack jumping from the plane at which delamination was initiated ($0^\circ/45^\circ$) to the other adjacent interface plane ($45^\circ/0^\circ$) [19]. This mechanism is characteristic for complex layups with $0^\circ/\varphi$ interfaces [20, 21]. The presence of this mechanism can be confirmed by macroscopic observation of the specimen edge for the specimen with the $0^\circ/45^\circ$ interface, where ‘crack jumping’ is visible at 25 and 40 mm crack lengths in Figure 5B. A similar stair-shape propagation path was observed by Sebaey et al. [20] as well as by de Moraes et al. [17] for an analogous $0^\circ/90^\circ$ interface. The above mentioned stair-shape propagation path has an influence on the *R-curve* shape (Fig. 4). For interface $0^\circ/90^\circ$ the SERR for crack propagation increases significantly above the SERR values determined for the $0^\circ/0^\circ$ and $0^\circ/45^\circ$ layups. In addition, this relatively high SERR for crack propagation on the $0/90$ interface can be associated with a large number of bridging fibers, as shown in Figure 5C.

As Figure 5C presents, configuration $0^\circ/90^\circ$ is characterized by a complex crack front. Many ‘crack jumps’ are visible between initial delamination plane $0^\circ/90^\circ$ and the adjacent interface plane $90^\circ/0^\circ$ - similar to the $0^\circ/45^\circ$ specimen, but with a higher frequency. A similar stair-shape propagation path was observed by Sebaey et al. [20] as well as by de Moraes et al. [17] for an analogous $0^\circ/90^\circ$ interface. The above mentioned stair-shape propagation path has an influence on the *R-curve* shape (Fig. 4). For interface $0^\circ/90^\circ$ the SERR for crack propagation increases significantly above the SERR values determined for the $0^\circ/0^\circ$ and $0^\circ/45^\circ$ layups. In addition, this relatively high SERR for crack propagation on the $0/90$ interface can be associated with a large number of bridging fibers, as shown in Figure 5C.

The SERR values determined at the *NL* point - G_{NL} , as well as determined thanks to the *R-curves* - G_{VIS} and G_{PROP} , were calculated by the EBT method [13] and are shown in Table 1 and in Figure 6.

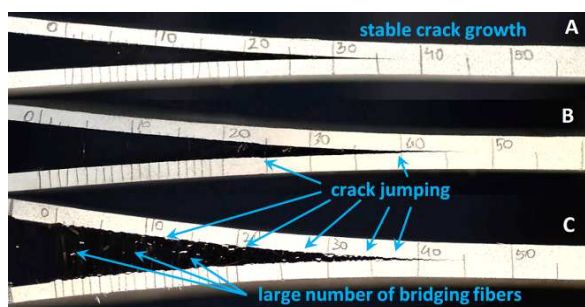


Fig. 5. Crack paths in composite with various interfaces: A - $0^\circ/0^\circ$; B - $0^\circ/45^\circ$; C - $0^\circ/90^\circ$

Rys. 5. Drogi rozwoju pęknięć w badanych interfejsach: A - $0^\circ/0^\circ$; B - $0^\circ/45^\circ$; C - $0^\circ/90^\circ$

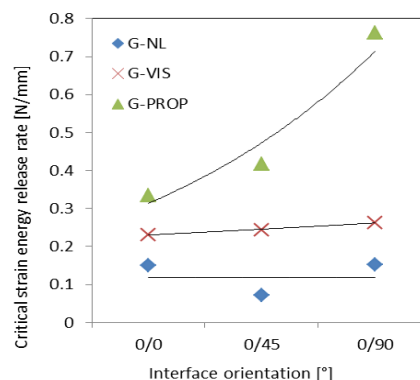


Fig. 6. Values of critical strain energy release rates for different criteria

Rys. 6. Wartości krytycznego współczynnika uwalniania energii dla różnych kryteriów

Based on the already determined SERR values by EBT, the mode mixity ratios (mode I/II) were calculated at the crack tip of multidirectional specimens, according to the method proposed Hutchinson and Suo [15]. The calculation results are presented in Table 1.

TABLE 1. Values of critical strain energy release rate for different criteria

TABELA 1. Wartości krytycznego współczynnika uwalniania energii dla różnych kryteriów

| | G_{NL} | G_{VIS} | G_{PROP} | mode mixity |
|--------------------|----------|-----------|------------|-------------|
| | [N/mm] | [N/mm] | [N/mm] | [°] |
| $0^\circ/0^\circ$ | 0.1509 | 0.2314 | 0.3346 | 0 |
| $0^\circ/45^\circ$ | 0.0719 | 0.2434 | 0.4162 | 2 |
| $0^\circ/90^\circ$ | 0.1514 | 0.2631 | 0.7621 | 2 |

Generally, based on the calculation results, it can be observed that for all of the tested layups, the SERR values for crack initiation criteria *NL* and *VIS* are very similar. Very small differences were observed especially for SERR calculated for the *VIS* points. The energy calculated for the *VIS* point is marked by G_{VIS} and indicates the energy causing the 1 mm crack increase.

The SERR value for the first nonlinear point of the *P-COD* curve - G_{NL} was slightly different for configuration $0^\circ/45^\circ$, which can be associated with a skew delamination front in laminates with non-zero *B* coupling extensional-bending stiffness [5, 21, 22]. The skew delamination front may cause the effect that the crack increase initiated on the opposite side of the specimen (not the observed edge of the specimen) would not be possible to observe macroscopically on one specimen edge until the skew delamination front increases along the axis of the sample [5].

CONCLUSIONS

In this paper, experimental Double Cantilever Beam tests were performed. Multidirectional laminates with

various fiber orientations were investigated. In the tests, force-crack opening displacement curves were recorded, as well on-line crack length measurements $a_0 + \Delta a$. Critical strain energy release rates were determined for different composite interfaces. Different crack onset criteria were taken into account - G_{NL} , G_{VIS} and G_{PROP} . On the basis of the performed experimental tests and analytical calculations, the following conclusions can be drawn:

- Mode I/II mixity at the crack tip is a variable for manufactured laminates. Homogeneous beams in configuration $0^\circ/0^\circ$ were characterized by pure mode I, whereas additional off-axis fiber layers resulted in the appearance of a slight shearing mode contribution (mode II).
- Similar values of SERR calculated for the first nonlinear point (NL) of the P -COD curve, as well as for macroscopic crack growth (VIS) - respectively G_{NL} , G_{VIS} , indicates that the energy causing crack initiation is rather a material constant and independent of the angular fiber orientation at the interface, which confirms the observations made by de Morais et al. [17].
- Fiber orientation in the composite interface is crucial to the SERR causing crack propagation - G_{PROP} . The highest SERR for crack propagation was observed for the $0^\circ/90^\circ$ specimen configuration, which is associated with a stair-shape propagation path and significant bridging effect. On the other hand, the lowest SERR for crack propagation was observed for the $0^\circ/0^\circ$ interface. The R -curve for the $0^\circ/45^\circ$ configuration had slightly higher energy levels than for $0^\circ/0^\circ$, with a clearly visible influence of 'crack jumping' which was observed macroscopically on the specimen edge.

REFERENCES

- [1] Hashin Z., Failure criteria for unidirectional fiber composites. *J. Appl. Mech.* 1980, 47, 329-334.
- [2] Hashin Z., Rotem A., A fatigue criterion for fiber-reinforced materials, *J. Compos. Mater.* 1973, 7, 448-464.
- [3] Puck A., Schürmann H., Failure analysis of FRP laminates by means of physically based phenomenological models, *Compos. Sci. Technol.* 1998, 58, 7, 1045-1067.
- [4] Bolotin V.V., Delaminations in composite structures: its origin, buckling, growth and stability, *Compos. Part B* 1996, 27B, 129-145.
- [5] Bieniaś J., Dadej K., Surowska B., Interlaminar fracture toughness of glass and carbon reinforced multidirectional fiber metal laminates, *Eng. Fract. Mech.* 2017, 175, 127-145.
- [6] Dadej K., Jakubczak P., Bieniaś J., Surowska B., The influence of impactor energy and geometry on degree of damage of glass fiber reinforced polymer subjected to low-velocity impact, *Composites Theory and Practice* 2015, 15, 3, 163-167.
- [7] Krause T., Tushev K., Koch D., Grathwohl G., Interlaminar Mode I crack growth energy release rate of carbon/carbon composites, *Eng. Fract. Mech.* 2013, 100, 38-51.
- [8] Davidson B.D., Kruger P., Konig M., Effect of stacking sequence on energy release rate distributions in multidirectional dcb and enf specimens, *Eng. Fract. Mech.* 1996, 55, 4, 557-569.
- [9] Schön J., Nyman T., Blom A., Ansell H., Numerical and experimental investigation of a composite ENF-specimen, *Eng. Fract. Mech.* 2000, 65, 4, 405-433.
- [10] Dadej K., Surowska B., Analysis of cohesive zone model parameters on response of glass-epoxy composite in mode II interlaminar fracture toughness test, *Compos. Theory and Practice* 2016, 16, 3, 180-188.
- [11] Andersons J., König M., Dependence of fracture toughness of composite laminates on interface ply orientations and delamination growth direction, *Compos. Sci. Technol.* 2004, 64, 13, 2139-2152.
- [12] Ducept F., Gamby D., Davies P., A mixed-mode failure criterion derived from tests on symmetric and asymmetric specimens, *Compos. Sci. Technol.* 1999, 59, 609-619.
- [13] Valvo P.S., On the calculation of energy release rate and mode mixity in delaminated laminated beams, *Eng. Fract. Mech.* 2016, 165, 114-139.
- [14] Jones R.M., *Mechanics of Composite Materials*, 2nd ed., Taylor & Francis, Philadelphia (PA) 1999.
- [15] Hutchinson J.W., Suo Z., Mixed mode cracking in layered materials, *Adv. Appl. Mech.* 1991, 29, 63-191.
- [16] ASTM D5528-13, Standard Test Method for Mode I Interlaminar Fracture Toughness of Unidirectional Fiber-Reinforced Polymer Matrix Composites, ASTM International, West Conshohocken, PA, 2013, www.astm.org
- [17] de Morais A.B., de Moura M.F., Marques A.T., de Castro P.T., Mode-I interlaminar fracture of carbon/epoxy cross-ply composites, *Compos. Sci. Technol.* 2002, 62, 679-686.
- [18] Ozdil F., Carlsson L.A., Beam analysis of angle-ply laminate DCB specimens, *Compos. Sci. Technol.* 1999, 59, 305-315.
- [19] Tohgo K., Hirako Y., Ishii H., Sano K., Mode I interlaminar fracture toughness and fracture mechanism of angle-ply carbon/nylon laminates, *J. Compos. Mater.* 1996, 3, 6, 650-661.
- [20] Sebaey T.A., Blanco N., Costa J., Lopes C.S., Characterization of crack propagation in mode I delamination of multidirectional CFRP laminates, *Compos. Sci. Technol.* 2012, 72, 1251-1256.
- [21] de Morais A.B., Double cantilever beam testing of multidirectional laminates, *Compos. Part A* 2003, 34, 12, 1135-1142.
- [22] Samborski S., Numerical analysis of the DCB test configuration applicability to mechanically coupled Fiber Reinforced laminated composite beams, *Compos. Struct.* 2016, 152, 477-487.